

## Tumour metabolites regulate tissue kallikrein in human umbilical vein endothelial cells

Naidoo, S.; Raidoo, D.; Mahabeer, R.; McLean, M.

*Published in:*  
Biochimica et Biophysica Acta - Molecular Cell Research

*DOI:*  
[10.1016/j.bbamcr.2003.12.007](https://doi.org/10.1016/j.bbamcr.2003.12.007)

Published: 03/05/2004

*Document Version:*  
Publisher's PDF, also known as Version of record

[Link to publication in Bond University research repository.](#)

*Recommended citation(APA):*  
Naidoo, S., Raidoo, D., Mahabeer, R., & McLean, M. (2004). Tumour metabolites regulate tissue kallikrein in human umbilical vein endothelial cells. *Biochimica et Biophysica Acta - Molecular Cell Research*, 1691(2-3), 117-127. <https://doi.org/10.1016/j.bbamcr.2003.12.007>

### General rights

Copyright and moral rights for the publications made accessible in the public portal are retained by the authors and/or other copyright owners and it is a condition of accessing publications that users recognise and abide by the legal requirements associated with these rights.

For more information, or if you believe that this document breaches copyright, please contact the Bond University research repository coordinator.

# Tumour metabolites regulate tissue kallikrein in human umbilical vein endothelial cells

S. Naidoo<sup>a,\*</sup>, D. Raidoo<sup>b</sup>, R. Mahabeer<sup>a</sup>, M. McLean<sup>c</sup>

<sup>a</sup>Department of Clinical and Experimental Pharmacology, Nelson R Mandela School of Medicine, Private Bag 7, Congella 4013, Durban, South Africa

<sup>b</sup>Division of Health Sciences, University of South Dakota, 57069 Vermillion, SD, USA

<sup>c</sup>Physiology, University of Natal Nelson R Mandela School of Medicine, 4000 Durban, South Africa

Received 12 September 2003; received in revised form 23 December 2003; accepted 23 December 2003

## Abstract

Angiogenesis, the sprouting of new blood vessels, is tightly mediated via a myriad of endogenous factors. A pro-angiogenic alteration facilitates the formation of neovascular tumour networks, thereby providing mechanisms for uncontrolled growth. The kallikrein–kinin system is postulated to be pro-angiogenic since its components have been detected in both endothelial cells and tumour tissue. No studies have, however, focussed on the role of tissue kallikrein (TK) in human angiogenic endothelial cell–tumour interactions. This study has optimised a challenge model whereby endothelial cells are presented with neuroblastoma metabolites, and vice versa. Image analysis of immunoreactive TK revealed a dose-dependant, significant reduction of TK localisation within endothelial cells, while gene expression remained unchanged, the latter determined by *in situ* RT-PCR. Neuroblastoma cells, when challenged with endothelial cell metabolites, displayed no change in TK synthesis or localisation. Alterations in TK synthesis and/or storage by angiogenic endothelial cells may be mediated by tumour-released signals and possibly indicate a shift from a proteolytic to a mitogenic function of TK. The challenge model provides a relatively simple experimental system to study angiogenic factors in tumour–endothelial cell interaction, and is the first to localise both TK and its mRNA within angiogenic endothelial and tumour cells.

© 2004 Elsevier B.V. All rights reserved.

**Keywords:** Angiogenesis; Endothelial cell; Tissue kallikrein; Immuno-labelling; *In situ* RT-PCR; Tumour metabolite

## 1. Introduction

Normal growth and development of mammalian tissues require an adequate blood supply [1]. To ensure survival, cells must be within a diffusion limit distance of 100–200  $\mu\text{m}$  from blood vessels [2]. Similarly, a tumour cannot expand more than 1–2  $\text{mm}^3$  before nutrients and waste products become rate-limiting [3]. Therefore, as Folkman [4] postulated three decades ago, a tumour mass has an absolute requirement for neo-vascularisation in order to expand and propagate. Angiogenesis is a cascading bio-

logical process whereby new blood vessels are formed [5] either from dividing progenitor endothelial cells [6] or recruited from preexisting vasculature [7–9]. This cascade occurs physiologically during foetal development and female reproduction [8,10,11], pathophysiologically during wound healing, and pathologically during rheumatoid arthritis [12], diabetic retinopathies [11], duodenal ulceration, and the growth of solid and haematological tumours [13]. To entice neo-vessel formation, tumour tissue and other cells including macrophages, mast cells and lymphocytes (attracted to the tumour by chemotaxis) secrete pro-angiogenic factors [7], which include basic fibroblast growth factor (bFGF) [14,15], vascular endothelial growth factor (VEGF) [16–18], angiogenin, transforming growth factor  $\beta$  (TGF- $\beta$ ), thrombin, angiopoietin-1, pleiotropin and scatter factor, amongst others. A number of proteolytic components including the matrix-degrading metalloproteinase (MMP) family [19] and the serine proteases (e.g. kallikrein–kinin system) stimulate tumour invasion and angiogenesis [20].

*Abbreviations:* BK, bradykinin; CLS, cord-like structures; HK, kininogen; D5, domain 5 of kininogen; HKa, TK-cleaved HK; hK1, 'true' tissue kallikrein gene; NO, nitric oxide; TK, tissue kallikrein; Tu, tumour metabolites added to culture medium in challenge model; uPAR, urokinase plasminogen activator receptor

\* Corresponding author. Tel.: +27-31-2604486/4334; fax: +27-31-2604338.

E-mail address: [naidoot@nu.ac.za](mailto:naidoot@nu.ac.za) (S. Naidoo).

Tissue kallikrein (TK) processes precursors to metalloproteinases, which are required for extracellular matrix (ECM) remodelling [21], and in vivo, TK activates progelatinase, an MMP involved in tumour mobility [21,22]. The release of TK in vivo can activate ECM-dependant proteolysis, and TK mRNA has been demonstrated on cultured bovine angiogenic endothelial cells [23]. In a recent in vitro study by Yayama et al. [24], the TK gene was found to be transcribed, expressed and secreted into the medium of both human umbilical vein endothelial cells (HUVECs) and human coronary artery endothelial cells. These and other studies have investigated the kallikrein–kinin system (KKS) in vascular endothelial cells and various tumours, but few, if any, have addressed the role of TK in the direct interaction between angiogenic endothelial cells and tumour cells. This study proposes a model to investigate the regulation of TK expression in endothelial cells when directly challenged with tumour cell metabolites. The aim was to qualitatively and quantitatively determine TK gene expression and protein translation, respectively, in an in vitro HUVEC/neuroblastoma model. This involved developing a challenge model, the use of in situ reverse transcriptase polymerase chain reaction (IS RT-PCR) to detect TK gene expression and the localisation of TK using polyclonal antibodies.

## 2. Materials and methods

### 2.1. Cell culture

The endothelial cell growth medium, designated EBM<sup>®</sup>-2 Bulletkit comprised basal medium (modified MCDB131), supplemented with human recombinant epidermal growth factor (hEGF), human fibroblast growth factor (hFGF), VEGF, ascorbic acid (vitamin C), hydrocortisone, human recombinant insulin-like growth factor (long R3-IGF-1), heparin, foetal bovine serum (FBS), gentamycin and amphotericin B. Tumour cell growth medium consisted of Dulbecco's modified Eagle's medium (DMEM) supplemented with 10% FBS, 100 µg/ml penicillin/streptomycin/fungizone (PSF), 2 mM L-glutamine (L-Glut), 2 mM sodium pyruvate and 3 µg/ml vancomycin. Neuroblastoma cells were initially grown in this supplemented DMEM before being weaned onto EBM<sup>®</sup>-2. All cell culture reagents were purchased from BioWhittaker, Walkersville, USA with the exception of L-Glut (Sigma Chemical, St. Louis, USA).

### 2.2. Cell lines

HUVECs were obtained as primary cultures (Clonetics, BioWhittaker), while the immortal neuroblastoma line (designated N2α) was obtained from Highveld Biological, National Repository for Biological Material of the Cancer Association of South Africa, Sandringham, South Africa.

### 2.3. Passaging conditions

HUVECs and N2α were seeded onto 60-mm culture dishes (Corning Costar, USA) at  $5 \times 10^3$  and  $1 \times 10^3$  cells/cm<sup>2</sup>, respectively, proliferated, harvested and passaged according to supplier's instructions. Only cell lines between passages 3 and 9 were used.

### 2.4. Challenge model

HUVECs and N2α cells were plated onto 8-well chamber slides (Iwaki, Japan), allowed to grow until approximately 60–70% confluent (typically 6–8 days), with fresh medium changes initially after 24 h and then every 48 h. Spent medium was extracted from one cell line, filtered through 0.22-µm syringe filters (Millex<sup>®</sup>, Millipore, USA), mixed in 10%, 25% and 50% ratios with fresh medium (mixture termed “challenge medium”) and used to feed the other cell line, and vice versa. In this way, metabolites released by one proliferating cell line were presented to the other proliferating cell line, in a dose-controlled manner. A maximum of 50% challenge medium dosage was determined to be the limit beyond which deleterious effects to cell health and growth were observed (retraction of peripheral cell membrane structures, rounding-off of cell bodies and retardation of growth and mitosis, as well as disintegrations of some cell membranes). The cells were exposed to the challenge medium for 24 h before being (serum-) cleared with serum-free medium. After 20 h of incubation, the cells were rinsed in cold Hanks Balanced Salt Solution (HBSS, Mg<sup>2+</sup> and Ca<sup>2+</sup>-free) and fixed in acetone/methanol (1:9, v/v) for 20 min at –20 °C. Chamber slides were stored at 4 °C, under RNase-free conditions, until immunochemistry and mRNA assays could be performed.

### 2.5. TK immunochemistry

Bovine serum albumin (BSA) and Milk Blocker<sup>®</sup> (casein protein) were obtained from Roche Molecular Biochemicals, Mannheim, Germany. The avidin–biotin (ABC) immunostaining kit (LSAB<sup>®</sup> plus), liquid DAB kit, von Willebrand's Factor (vWF) and cytokeratin 19 (CK19) antibodies were purchased from Dako, UK. The primary antibody, an anti-human polyclonal goat IgG raised against a recombinant human TK, was isolated and fully characterised for specificity and sensitivity, as previously described [25].

#### 2.5.1. Procedure

Challenged HUVECs and N2α cells (from challenge model section above) were fixed in acetone/methanol (1:9, v/v) for a further 5 min at –20 °C, incubated in Tris-buffered saline (TBS, 150 mM NaCl, 50 mM Tris, pH 7.5) for 5 min, and further incubated for 15 min in 7% BSA/TBS (w/v), at room temperature (RT). Nonspecific sites on the cells were blocked with 10% Milk Blocker<sup>®</sup>, diluted in 7%

BSA/TBS (v/v), for 30 min at RT. Cells were incubated with primary antibody (TK, CK19 and vWF were all diluted 1:100 in 10% Milk Blocker®) under humid conditions, overnight at 4 °C. 10% Milk Blocker® was used to replace the primary antibody for the negative control. Subsequently, cells were washed with TBS and conjugated to a multi-species biotinylated linker antibody, which was coupled to horse-radish peroxidase–streptavidin complex (LSAB® plus) according to manufacturer's instructions, at RT. The reaction was precipitated with 3, 3'-diaminobenzidine (DAB). The slides were counter-stained with haematoxylin, dehydrated through a dilution series of alcohol into xylene, and finally mounted with nonaqueous mountant.

The method control used was paraffin-embedded normal human submandibular gland, a known source of TK [26]. The tissue was probed for the presence of TK, according to established immunocytochemistry protocols [27]. For negative controls, the primary antibody was omitted and replaced with 10% Milk Blocker®.

Results were viewed using a Leica DMLB bright-field/phase-contrast microscope coupled to a Leica DC100 digital camera (Leica, Heidelberg, Germany). 24-bit tagged image format (TIFF) images were captured and converted to 8-bit black and white images to enable regions of interest to be selected. The grey scale intensity of specific label in the digitised images was quantified using AnalySIS Pro image analysis software (Soft Imaging Systems, Germany) using predetermined threshold range-limited pixel/ $\mu\text{m}^2$  values.

## 2.6. *In situ* reverse-transcriptase polymerase chain reaction (IS RT-PCR)

First Strand cDNA Synthesis Kit™ was purchased from Amersham Pharmacia Biotech, Buckinghamshire, UK. DIG RNA Labelling Kit®, Proteinase K, nitroblue tetrazolium/5-bromo-chloro-indoyl-phosphate (NBT/BCIP), DIG Wash and Block Set® (containing Milk Blocker®, 10 × detection buffer and maleic acid) and sheep anti-digoxigenin (DIG) alkaline phosphatase-conjugated IgG were obtained from Roche. Unless otherwise indicated, all solutions were made up in 1% DEPC-dH<sub>2</sub>O (v/v). Synthetic TK RNA primers hKLK1-160F [10 mM, 21-mer (5'-CTG TAC CAT TTC AGC ACT TTC-3')], hKLK1-742R [10 mM, 17-mer (5'-GCC ACA AGG GAC GTA GC-3')] and hKLK1-790R [10 mM, 21-mer, (5'-TCA CAT AAG ACA GCA CTC TGA-3')] were obtained from MWG-Biotech AG, Ebersberg, Germany. Gene Frame® incubation chambers were purchased from Advanced Biotechnologies, Surrey, UK.

### 2.6.1. Pretreatment

HUVECs and N2α from the challenge experiments were fixed in freshly prepared 4% paraformaldehyde for 20 min at RT and then rinsed three times in TBS. Next, partial protein digestion of the cells was performed in 0.01 M HCl for 10 min at RT. The walls of the chamber slides were manually removed and 65- $\mu\text{l}$  incubation chambers

were placed around each well to create an isolation chamber. Cell membranes were partially permeabilised by Proteinase K digestion for 20 min at 37 °C. Based on a concentration range of 0.5 to 50  $\mu\text{g}/\text{ml}$ , an optimal concentration of 1  $\mu\text{g}/\text{ml}$  Proteinase K was considered to be the highest concentration at which cellular structure was not compromised. This was followed by extensive rinsing in cold TBS (3 × 10 min at 4 °C) to inactivate the enzyme. Cells were then dehydrated through a graded series of alcohol and air-dried.

### 2.6.2. Reverse transcriptase polymerase reaction (RT-PCR)

The reverse transcriptase solution was prepared according to the manufacturer's instructions using the First Strand cDNA Synthesis Kit® and the reverse primer hKLK1-790R. Briefly, for each reaction, a mix containing 4- $\mu\text{l}$  10  $\mu\text{M}$  dithiothreitol (DTT), 4- $\mu\text{l}$  hKLK1-790R reverse primer, 44- $\mu\text{l}$  DEPC-dH<sub>2</sub>O, and bulk kit mix (without Ca<sup>2+</sup> and Mg<sup>2+</sup>) was prepared. Sixty microliters of this reaction mixture was placed onto the cells in each incubation chamber and the chamber covered with a plastic coverslip. Slides were placed in the humid chamber of a Hybaid OmniSlide Flatblock (Hybaid, Middlesex, UK) and incubated at 37 °C for 150 min.

The spent reaction mixture was then carefully removed and replaced with 60  $\mu\text{l}$  of the PCR1 mixture containing 5- $\mu\text{l}$  10 × Taq buffer (with MgCl<sub>2</sub>), 2  $\mu\text{l}$  each of hKLK1-160F and hKLK1-790R primers, 1- $\mu\text{l}$  Taq DNA polymerase (5 U/ $\mu\text{l}$ ), 10- $\mu\text{l}$  10 mM dNTP mix and 40- $\mu\text{l}$  DEPC-dH<sub>2</sub>O. A plastic coverslip was placed over the cells and the incubation chamber sealed to prevent the cells from dehydrating. Thermal cycling was performed on a Hybaid OmniSlide Flatblock using the following conditions: initial denaturation (92 °C for 2 min), followed by 15 cycles of denaturation (92 °C for 1 min each), annealing (55 °C for 1 min) and extension (72 °C for 1 min), and a final extension (72 °C for 2 min). The PCR1 mixture was then carefully removed and replaced with 60  $\mu\text{l}$  of the PCR2 mixture containing 5- $\mu\text{l}$  10 × Taq buffer (with MgCl<sub>2</sub>), 2  $\mu\text{l}$  each of hKLK1-160F and hKLK1-742R, 1- $\mu\text{l}$  Taq DNA polymerase (5 U/ $\mu\text{l}$ ), 10- $\mu\text{l}$  10 × PCR DIG labelling mix (DIG RNA Labelling Kit®) and 30- $\mu\text{l}$  dH<sub>2</sub>O. Again, a plastic coverslip was placed over the incubation chamber and sealed. Thermal cycling was performed as follows: initial denaturation (92 °C for 2 min), followed by five cycles of denaturation (92 °C for 1 min each), annealing (55 °C for 1 min) and extension (72 °C for 1 min), and a final extension (72 °C for 2 min).

After thermal cycling, the coverslip was carefully removed and the tissue washed in 2 × saline sodium citrate (SSC) at 37 °C for 30 min, 1 × SSC at 55 °C for 20 min, 0.5 × SSC at 55 °C for 20 min and finally in 0.5 × SSC at 55 °C for 20 min. Negative control reactions were also carried out in which the primers were omitted from the reverse transcriptase and PCR reactions and the final volume of the solutions compensated with DEPC-dH<sub>2</sub>O.

### 2.6.3. Immuno-detection of digoxigenin-labelled amplifiants

Following the SSC washes, the slides were washed twice in TBS and blocked with 10% blocking reagent, (DIG Wash and Block Set®) for 15 min at RT. The cells were then incubated with a polyclonal sheep anti-DIG IgG alkaline phosphatase conjugate, diluted 1:500 in 10% blocking reagent, overnight at 4 °C. Slides were washed twice in TBS and covered with a freshly prepared NBT/BCIP solution, diluted 1:50 in 1 × detection buffer (DIG Wash and Block Set®). The chromogen was allowed to develop in the dark at RT, until a purple-black-coloured precipitate was distinct. The slides were washed extensively in tap water, counter-stained with haematoxylin, dehydrated and mounted. Results were viewed using a Leica DMLB bright-field/phase-contrast microscope coupled to a Leica DC100 digital camera.

### 2.7. Statistical analysis

All data obtained from image analysis of immunoreactive TK-labelled cells in the challenge model (see TK immunocytochemistry section above) were expressed as mean ± S.D. (Fig. 2). All labelling experiments were done in triplicate. For images to be analysed, at least five fields in each experiment were selected and imaged, and cells in these were selected approximately for size and shape. The Student's *t* test (unequal variance) was used to assess statistical significance ( $P < 0.05$ ).

## 3. Results

### 3.1. Phenotypic growth profiles of cells in the challenge model

The phenotypic profile of unchallenged HUVECs showed initial lag-phase growth after seeding, followed by exponential growth. Cells in close proximity to one another extended tentative pseudopodia-like sprouts. Three to four days after initial seeding, some cord-like structures (CLS) were established with cells lining up end-on-end. By the 5th to 6th day post-seeding, 60–70% sub-confluency, in addition to CLS, was noted. In the challenge model, no considerable number of HUVECs or N2α succumbed to necrosis (complete disintegration of cell membranes) or apoptosis (retraction of peripheral cell membrane structures, membrane blebbing or “rounded-off”, condensation of nuclei). The visual growth of HUVECs, subjectively compared to non-challenged cells, did not appear to be markedly different in response to the tumour cell metabolite concentrations [Tu].

N2α cells grown on two-dimensional surfaces did not exhibit CLS, but instead formed monolayer clusters at sub-confluency, with cells appearing fibroblastic. The different endothelial cell metabolite concentrations [En] in the chal-

lenge model did not appear to alter the growth patterns or growth rate of the N2α cells.

### 3.2. Immunochemical staining for TK

#### 3.2.1. Immunocytochemistry controls

The TK positive method control showed labelling within the duct-lining epithelial cells but not the acini in the submandibular gland (Fig. 1a) [25,26,28]. Unchallenged HUVECs and N2α cells served as cell culture controls. Positive DAB staining was observed within HUVECs (labelled with vWF) and N2α (labelled with CK-19), respectively (Fig. 1b and c). In the method controls the primary antibody (TK, vWF or CK-19) was replaced with dilution buffer, and both HUVECs and N2α showed no nonspecific label (Fig. 1d and e). To confirm endothelial cell function in the challenge model, 50% challenged HUVECs demonstrated vWF labelling (Fig. 1f) that was similar to the unchallenged endothelial cells (Fig. 1b).

#### 3.2.2. TK immunoreactivity in unchallenged HUVECS

This aspect of the model served as the cell culture control, since these endothelial cells were not exposed to challenge medium. Unchallenged HUVECs at the periphery of the sub-confluent growth areas demonstrated extensive TK labelling, especially within the cytoplasm of cells (Fig. 1g). TK localisation was most convincing on the leading edges of advancing cells that presented cell-to-cell contact extensions, or locomotor extensions along the growth surface. Cells maintaining CLS exhibited TK mainly in the cell body structures. Visually, approximately 40% of unchallenged HUVECs, per microscopic field, specifically labelled for TK.

#### 3.2.3. TK in challenged HUVECS

Decreased TK immuno-detection patterns emerged as the [Tu] delivered to HUVECs increased. TK labelling in the 10% challenged HUVECs was observed along cells forming CLS, while some HUVECs that formed confluent regions did not label at all (Fig. 1h). HUVECs incubated with the 25% challenged medium also demonstrated TK immuno-label along the CLS in the cytoplasm and extensions between cells (Fig. 1i). The 50% challenged HUVECs visually demonstrated a reduced perinuclear labelling intensity (Fig. 1j). The increase in [Tu] thus appeared to elicit a decrease in TK immuno-localisation in endothelial cells.

Image analysis revealed a reduction in the staining intensity gradients with increasing [Tu] concentrations (Fig. 2a). Despite this reduction in immunoreactive TK, there was no visible alteration of the growth/proliferation patterns of challenged HUVECs when compared with growth patterns of unchallenged HUVECs. ‘Rounding off’ of endothelial cells in culture due to retraction of extensions and condensation of nuclei, visual markers of apoptosis, was not markedly increased, and did not favour either challenged or unchallenged HUVECs.

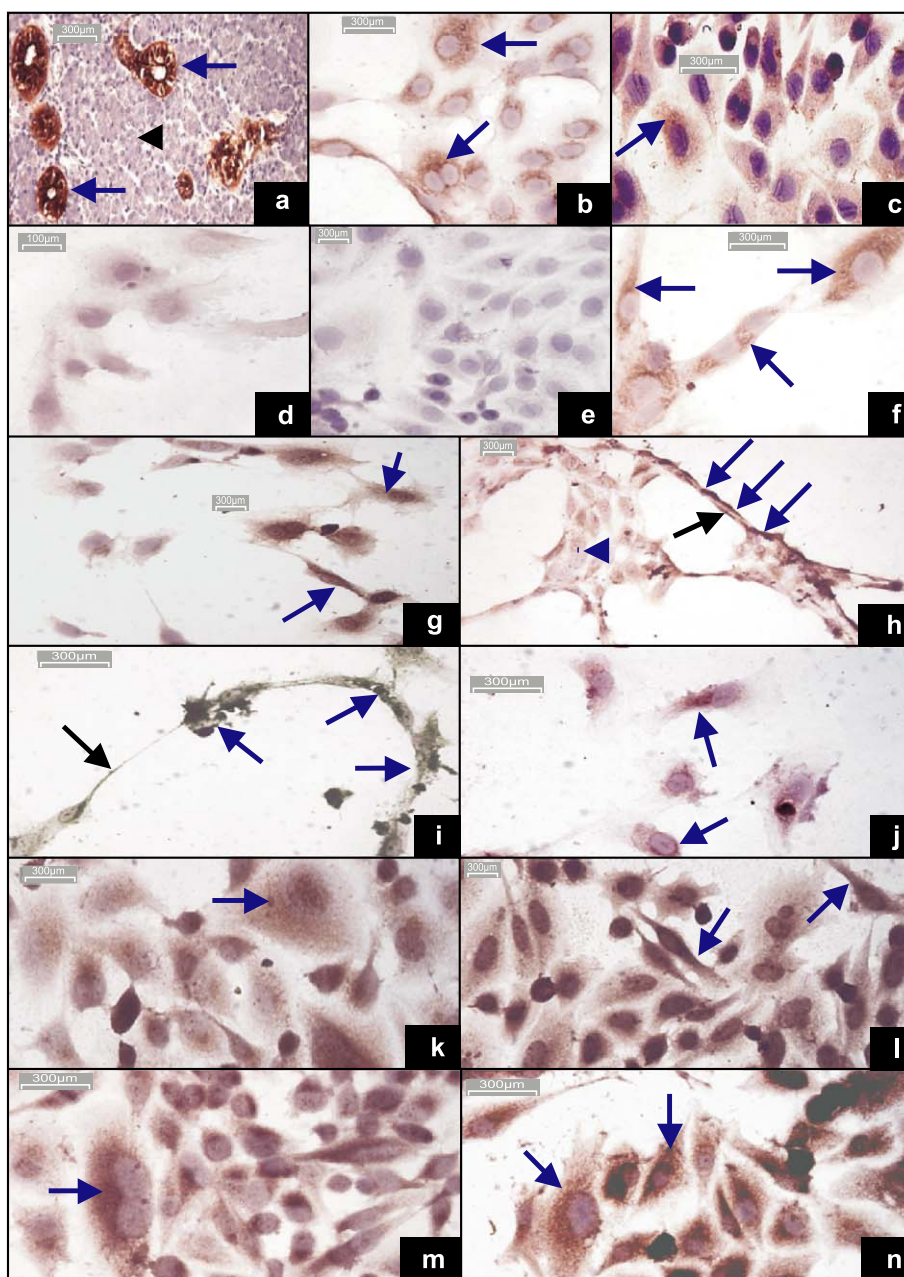


Fig. 1. Immunohistochemical changes in the challenge model. Positive label is depicted as a brown precipitate (DAB), and scale bars on each image = 300  $\mu$ m. Normal human submandibular gland, used as TK positive tissue control (Fig. 1a,  $\times 200$ ), demonstrated labelling in glandular structures (blue arrows) and an absence of label within the acini (black arrowhead). HUVEC and N2 $\alpha$  positive cell culture controls demonstrated vWF and CK-19 label (blue arrows) in b ( $\times 400$ ) and c ( $\times 400$ ), respectively. HUVEC and N2 $\alpha$  negative cell culture method controls demonstrated complete absence of TK in d ( $\times 400$ ) and e ( $\times 400$ ), respectively. To verify that endothelial cell function was retained, perinuclear staining for vWF (blue arrows) was demonstrated in 50% challenged HUVECs (f,  $\times 400$ ). In the HUVEC challenge model, TK staining (blue arrows) was demonstrated within unchallenged HUVECs (g,  $\times 400$ ) and challenged HUVECs [(10%, h,  $\times 200$ ), (25%, i,  $\times 400$ ) and (50%, j,  $\times 400$ )]. Examples of CLS formation are demonstrated in h and i (black arrows). Also note the absence of label in an adjacent semi-confluent region (h, blue arrowhead). In the N2 $\alpha$  challenge model, TK immunolabelling (blue arrows) was demonstrated within unchallenged N2 $\alpha$  [(10%, k,  $\times 400$ ) and (25%, l,  $\times 400$ )], (25%, m,  $\times 400$ ) and (50%, n,  $\times 400$ ). Note an actively dividing cell with perinuclear staining (m, blue arrow).

#### 3.2.4. TK in unchallenged and challenged N2 $\alpha$

Unchallenged N2 $\alpha$  demonstrated TK staining in the cytoplasm of most cells (Fig. 1k). The increase in [En] did not appear to potentiate or diminish TK labelling [Fig. 1l (10% challenged), Fig. 1m (25% challenged) and Fig. 1n (50% challenged)]. Challenged N2 $\alpha$  cultures did not

exhibit any alteration in growth response to [En]. In both the challenged and unchallenged models, cells that grew in isolation displayed TK within their entire cell bodies, while cells that were undergoing mitosis (Fig. 1m and n) or exhibiting extensor-like projections showed perinuclear localisation of TK.

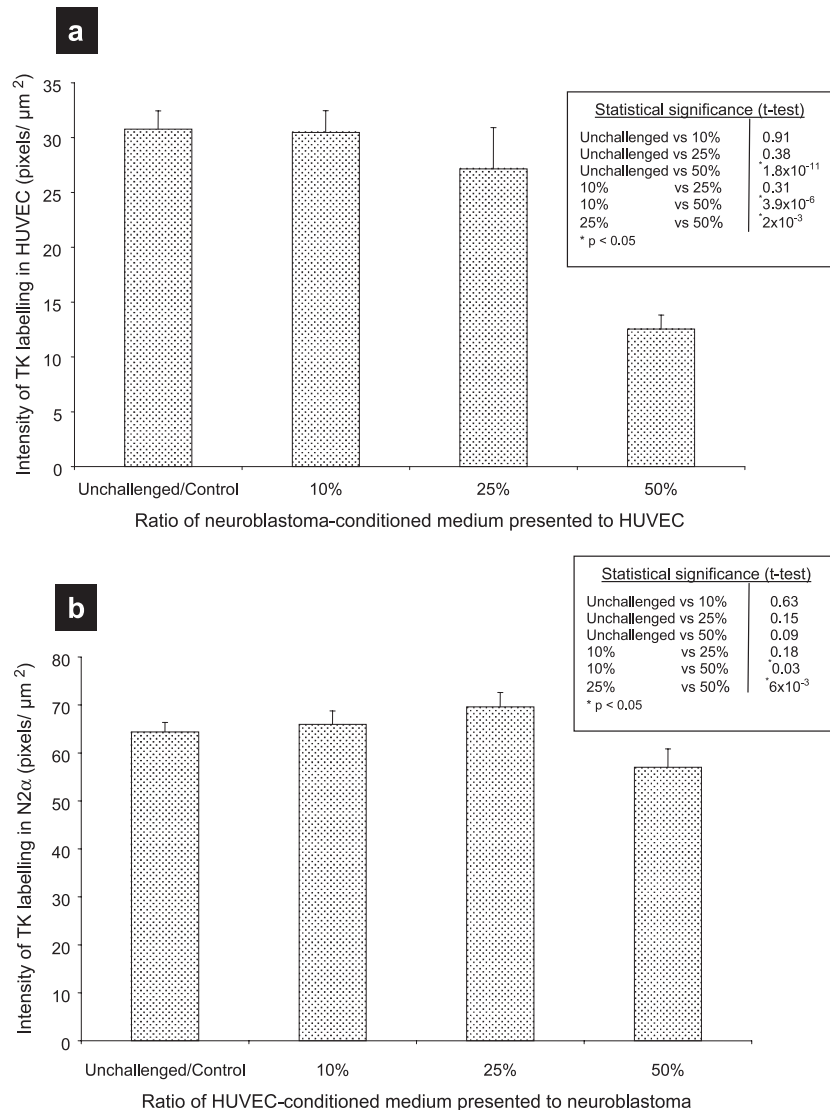


Fig. 2. Dose-dependent effects of metabolites on TK label-intensity in HUVECs and N2 $\alpha$  in the challenge model. (a) depicts the dose-dependant effects of tumour metabolites on the labelling intensity of TK, when presented to HUVECs; while (b) represents the dose-dependant effects of HUVEC metabolites on the labelling intensity of TK within N2 $\alpha$ . Digital image analysis of TK-DAB labelling intensity of unchallenged cells was statistically compared with conditioned medium challenged cells (shown in separate text blocks for both a and b). Statistical significance was represented by  $P < 0.05$ .

### 3.2.5. Image analysis

Image analysis histograms of TK labelling intensities (Fig. 2a and b) indicated a statistically significant decrease when 50% challenged HUVECs were compared with unchallenged HUVECs ( $P = 1.8 \times 10^{-11}$ ), 10% challenged HUVECs ( $P = 3.9 \times 10^{-6}$ ) and 25% challenged HUVECs ( $P = 2 \times 10^{-3}$ ). Thus, the overall trend appeared to be a significant decrease in TK immunoreactivity as the HUVECs became increasingly challenged with medium containing tumour metabolites.

The dose-dependent effect of HUVEC-conditioned medium did not statistically change the mean labelling intensities of the exposed neuroblastoma cells, except between the 25% and 50% challenged N2 $\alpha$  ( $P = 6 \times 10^{-3}$ , Fig. 2b). There was, in fact, a slight increase in mean TK intensity as the [En] ratio increased to 25%, but the difference was not

statistically significant. Therefore, there did not appear to be an altered regulation of TK within neuroblastoma cells challenged with [En].

### 3.3. IS RT-PCR

#### 3.3.1. Controls

In the human submandibular gland tissue method control, positive label for TK mRNA was demonstrated in the cytoplasm of the duct cells (Fig. 3a). In the negative tissue method control, the reverse primer hKLLK-790R was omitted during reverse transcriptase, and so were both reverse (hKLLK-742R) and forward (hKLLK-160F) primers during PCR. Thus, in the negative method controls, there was an absence of TK mRNA label in the cytoplasm of the duct cells but some artifactual labelling of nuclei (Fig. 3b). This

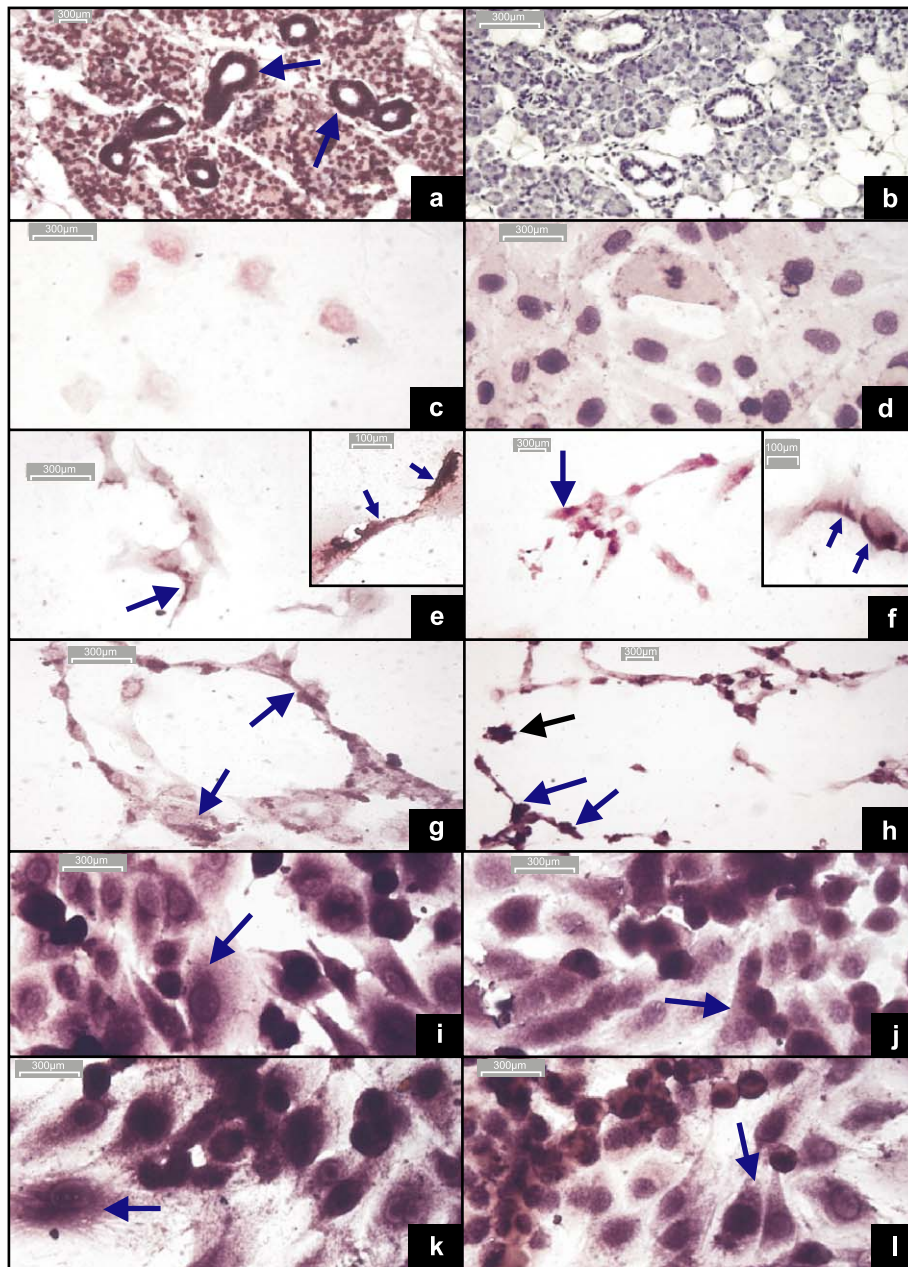


Fig. 3. Detection of TK mRNA by IS RT-PCR. TK mRNA was visually represented by a purple/black precipitate, and scale bars on each image = 300  $\mu$ m. Human submandibular gland positive method control (a,  $\times 200$ ) demonstrated cytoplasmic TK mRNA in duct cells (blue arrows), while the negative method control showed a lack of TK mRNA cytoplasmic staining (b,  $\times 200$ ). Artfactual labelling observed within the nuclei (visually distinct in negative control, d) was due to nicked nuclear DNA fragments, cleaved by DNase, being repaired by Taq DNA polymerase, and incorporating DIG-dUTP into the repaired DNA, which was subsequently observed as nonspecific labelling within the nuclei in both method controls and positively labelled cells. HUVEC and N2 $\alpha$  cell culture negative controls [c ( $\times 400$ ) and d ( $\times 400$ ), respectively] demonstrated an absence of cytoplasmic TK mRNA, in which all primers were omitted in both the reverse transcriptase and PCR reactions. TK mRNA labelling (blue arrows) was demonstrated within unchallenged HUVECs [(endothelial cell culture positive control); e,  $\times 400$ ], challenged HUVECs [(10%, f,  $\times 200$ ), (25%, g,  $\times 400$ ) and (50%, h,  $\times 200$ )]; as well as in unchallenged N2 $\alpha$  [(tumour cell culture positive control); i,  $\times 400$ ] and challenged N2 $\alpha$  [(10%, j,  $\times 400$ ), (25%, k,  $\times 400$ ) and (50%, l,  $\times 400$ )]. (h) demonstrated cells clumping together and extensive label over the entire cell body (black arrow). Note that insets in e ( $\times 400$ ) and f ( $\times 400$ ) demonstrate peripheral mRNA label in individual endothelial cells (blue arrows).

was due to nonspecific nuclear labelling occurring during the PCR reaction whereby the Taq DNA polymerase is known to screen nuclear DNA for nicks caused by DNase, and repair these fragments. In doing so, DIG-dUTP from the nucleotide pool would be incorporated into the repaired

nuclear strands and this would account for the nonspecific nuclear labelling in both the negative and positive control tissue. Tissue culture negative method controls for HUVECs and N2 $\alpha$  cells also demonstrated no cytoplasmic mRNA labelling, although nonspecific nuclear staining was evident



(Fig. 3c and d, respectively). The unchallenged HUVEC and N2 $\alpha$  cells served as positive cell culture controls for IS RT-PCR and both cell types demonstrated TK mRNA label within their cytoplasm (Fig. 3e and i).

### 3.3.2. TK mRNA in HUVECS

Both unchallenged (Fig. 3e) and challenged HUVECs [Fig. 3f (10%), g (25%) and h (50%)] exhibited cytoplasmic TK mRNA, and nonspecific nuclear labelling. There was no differing pattern of mRNA labelling amongst the various challenged cells, and while most HUVECs demonstrated cytoplasmic label (Fig. 3e and f), many also showed label along the cell body periphery (insets, Fig. 3f and g) and not in the cellular extensions. This could be due to the presence of transcriptional machinery within the cell body rather than the cellular extensions. In areas of cell clumping, the mRNA appeared to be spread throughout the cell body (Fig. 3h), possibly reflecting the effect of overgrowth. CLS did not exhibit atypical label patterns compared with individual cells (Fig. 3g). In general, no differing intensity of TK mRNA label could be ascertained possibly because this type of IS RT-PCR is not quantitative. The ratio of labelled cells to total cells was determined by taking the mean of five different fields of view, for each challenge and counting the cells. This approximation revealed the presence of TK mRNA in 30% to 50% of both unchallenged and challenged HUVECs.

### 3.3.3. TK mRNA in neuroblastoma cells

The extent and intensity of mRNA localisation in N2 $\alpha$  cells appeared to be greater than that observed in HUVECs. Within N2 $\alpha$  cells there was no discernable difference in the pattern of staining between the unchallenged (Fig. 3i) and challenged cells [Fig. 3j (10% challenged), Fig. 3k (25% challenged) and Fig. 3l (50% challenged)], and cytoplasmic TK mRNA label was found in virtually all cells, irrespective of whether they were solitary or in close contact with each other. In addition, the cellular localisation of TK mRNA extended throughout the cell body and the extensor regions.

## 4. Discussion

TK processes high and low molecular weight kininogen (HK/LK) to liberate the bioactive kinin peptides, bradykinin (BK) and kallidin. The actions of kinins result in the production of nitric oxide (NO) and prostacyclin (PGI<sub>2</sub>) [26] which increase vascular permeability and cause vasodilation [29]. Kinins are also known to promote cell proliferation and tissue regeneration by influencing DNA synthesis and mitosis [30]. This present study has successfully demonstrated both immunoreactive TK and TK mRNA within the cytoplasm of angiogenic endothelial cells and neuroblastoma cells, indirectly interacting in culture. These results corroborate prior work where the TK gene was

shown to be expressed and secreted in both HUVECs and human coronary artery endothelial cells [24]. In addition, TK has been previously shown in various tumour cells of the breast [31], oesophagus [32], pituitary [33], astrocytes [34] and cultured gastric carcinoma cells [35]. Recent studies have demonstrated TK mRNA on bovine angiogenic endothelial cells [23] and non-angiogenic HUVECs [24]. The present study introduces new findings that demonstrate TK mRNA transcription within angiogenic endothelial cells and N2 $\alpha$  cells in culture.

The challenge model demonstrates that as the [Tu] in the HUVEC medium increases, there is a significant decrease in immunoreactive TK labelling. This may be due to one or a combination of the following effects of tumour metabolites on endothelial cells: (i) a reduction in TK synthesis; (ii) an increase in TK secretion (experiments are currently underway to examine this hypothesis); and/or (iii) accelerated conversion of pro-TK to active TK, leading to an increase in kallikrein functional activity and a subsequent decrease in immunoreactive TK due to half-life turnover (Fig. 4). The latter effect is supported by the ability of TK to act as a mitogen [30] and as a protease in ECM degradation.

The TK-secretion supposition may be answered, in part, by a study by Stadnicki et al. [36], who have shown that there is a significant decrease in TK secretion by granulomatous cecal tissue, in culture, in an enterocolitis-induced rat model. Further, they reported no significant alteration in intestinal TK mRNA levels but decreased plasma levels of kallikrein-binding protein (a rat analogue of kallistatin, a TK inhibitor). Thus, they postulated that significant amounts of TK would have been released *in vivo* by the cells during inflammation. In a later study advocating TK release, Stadnicki et al. [37] have found a significant decrease in TK levels in inflamed human intestinal tissue in ulcerative colitis and Crohn's disease. Since this present study indicates no change in TK mRNA transcription, at this point it may be presumed that the decrease in immunoreactive TK is not due to a decrease in TK synthesis.

TK activates pro-gelatinases [21] and processes pro-metalloproteinases required for ECM remodelling [22], and thus lends itself to a role in promoting tumour invasiveness. The serine proteinase inhibitor (serpin) kallistatin has been found to inhibit angiogenesis, both *in vivo* and *in vitro* [38], and this supports a pro-angiogenic function for TK. Further, the inhibition of TK using a synthetic inhibitor has also been shown to suppress *in vitro* tumour invasiveness [39].

High-molecular weight kininogen (HK) can specifically bind to endothelial cells, which then serves as a receptor complex for prekallikrein binding, and the activation of the latter to kallikrein results in the release of bradykinin (BK) from HK and the formation of kallikrein-cleaved HK (HKa). It was also demonstrated that HKa competitively binds to domains 2 (D2) and 3 (D3) of the urokinase plasminogen activator receptor (uPAR)—an adhesion receptor for vitronectin [40]. Asakura et al. [41] showed that HKa is anti-

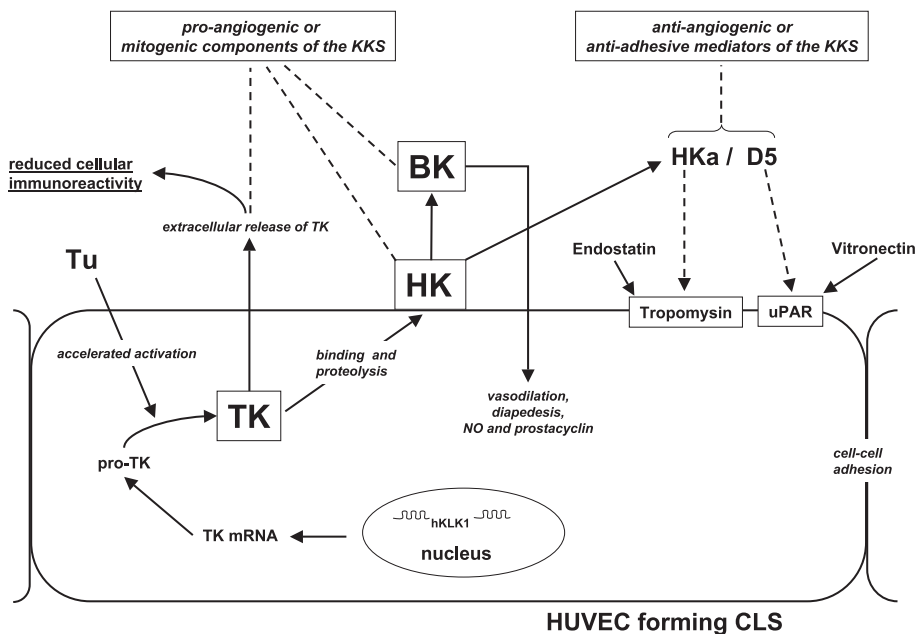


Fig. 4. Proposed subcellular effects of tumour metabolites on TK in HUVECs. Neuroblastoma tumour metabolites may cause accelerated activation of pro-TK to functional TK in challenged HUVECs, resulting in increased proteolytic release of BK from HK, with no concomitant change in TK gene expression. This, together with extracellular release of pro-angiogenic TK, possibly accounts for the reduced cellular immunolocalisation of TK. TK, BK, as well as HK are pro-angiogenic, while HKa and HKa D5 are anti-angiogenic and anti-adhesive. The latter effects may be due to the competitive binding of HKa to uPAR (a vitronectin-adhesion receptor) and the actions of HKa D5 on the endostatin-associated, membrane-bound protein tropomyosin. Both active TK and BK can regulate tumour cell proliferation due to their mitogenic capacity.

adhesive in an endothelial/vitronectin model. Colman et al. [42], in a series of experiments, showed that D5 of HK as well as HKa inhibit endothelial cell proliferation and in vitro angiogenesis, whereas HK itself was not anti-angiogenic. Similar experiments by Zhang et al. [43] found that HKa and a specific HK D5 peptide, but not HK, low-molecular weight kininogen (LK), BK or BK antibodies, inhibited proliferation and induced apoptosis of endothelial cells in a  $Zn^{2+}$ -dependant manner. This is in contrast to a recent study by Colman et al. [44] who found that HK and LK (via BK release), and BK itself are pro-angiogenic. In addition, Zhang et al. [45] have found that in HKa-induced apoptosis, D5 is involved in binding to the surface-bound cytoskeletal protein tropomyosin, which has been shown to mediate the effects of the potent antiangiogenic factor endostatin, leading one to consider that HKa may also be involved in tropomyosin-mediated pro-angiogenic signal transduction events.

Challenged N2 $\alpha$  cells showed no alteration in TK mRNA transcription or TK synthesis, and endothelial cell metabolites appeared to have little or no effect on the rate of neuroblastoma cell proliferation. It was evident, however, that compared with endothelial cells there was a greater transcription of TK mRNA in N2 $\alpha$  cells, probably driven by extremely productive tumour genetic expression. This may explain the indiscriminate localisation of TK mRNA in neuroblastoma cell bodies, which did not necessarily favour peripheral sprouts. Thus, while not outwardly toxic to the neuroblastoma cells, the endothelial cells metabolites may

have some other effect on neuroblastoma cell metabolism. The ability of TK to up-regulate mitosis and DNA synthesis may be a consideration within aggressively proliferating tumour tissue.

This study has successfully set up a challenge model whereby tumour metabolites, released into the culture medium, are presented to human endothelial cells, without having a deleterious effect on cell viability. Since both tumour cells and endothelial cells are grown in the same culture medium, the effects of supplemented growth factors are negligible. In addition, the effect of serum proteins on the TK labelling can also be discounted since, prior to fixation, cells were serum-starved. A limitation of this model is the absence of an ECM and factors associated with it, since conformationally altered proteins (and their fragments) derived from ECM as well as other signalling cues have been reported to play a role in angiogenesis [45,46]. Another system currently being optimised is a three-dimensional basement membrane complex (Matrigel) applied to the challenge model. This will address the role of TK in HUVEC–tumour interactions supported by an ECM.

The interplay between endothelial cells and tumour cells in regulating TK warrants further investigation. Since kallikrein appears to have multi-faceted functions in tumorigenesis and angiogenesis, empirical models need to be established to clearly define these relationships. To conclude, the challenge model forms an important experimental mechanism in elucidating the role of protein systems in

angiogenesis, and applications could encompass a variety of candidate proteases and hormones.

## Acknowledgements

The authors wish to acknowledge the following South African institutions: the Medical Research Council (MRC), National Research Foundation (NRF), Cancer Association of South Africa (CANSAs) and the University of Natal for funding part/s of this project. The authors also thank Mrs. Celia Snyman for her technical expertise in the image analysis work.

## References

- [1] P. Carmeliet, Mechanisms of angiogenesis and arteriogenesis, *Nat. Med.* 6 (2000) 389–395.
- [2] P. Carmeliet, R.K. Jain, Angiogenesis in cancer and other diseases, *Nature* 407 (2000) 249–257.
- [3] B. Zetter, Angiogenesis and tumour metastasis, *Annu. Rev. Med.* 49 (1998) 407–424.
- [4] J. Folkman, Tumour angiogenesis: therapeutic implications, *New Engl. J. Med.* 285 (1971) 1182–1186.
- [5] S. Mousa, Angiogenesis: regulation and dysregulation, *Mol. Med. Today* 97 (1998) 101.
- [6] T. Asahara, T. Murohara, A. Sullivan, M. Silver, Z. Van der, T. Li, B. Witzendichler, G. Schatteman, J.M. Isner, Isolation of putative endothelial cells for angiogenesis, *Science* 275 (1997) 964–967.
- [7] R. Folberg, M.J.C. Hendrix, A.J. Maniotis, Vasculogenic mimicry and tumor angiogenesis, *Am. J. Pathol.* 156 (2000) 361–381.
- [8] W.J. Gradishar, An overview of clinical trials involving inhibitors of angiogenesis and their mechanism of action, *Invest. New Drugs* 15 (1997) 49–59.
- [9] L. Sun, G. McMahon, Inhibition of tumor angiogenesis by synthetic receptor tyrosine kinase inhibitors, *DDT* 5 (2000) 344–353.
- [10] S. Liekens, E.D. Clercq, J. Neyts, Angiogenesis: Regulators and clinical applications, *Biochem. Pharmacol.* 61 (2001) 253–270.
- [11] N. Ferrara, K. Alitalo, Clinical applications for angiogenic growth factors and their inhibitors, *Nat. Med.* 5 (1999) 1359–1364.
- [12] A. Koch, Angiogenesis: implications for rheumatoid arthritis, *Arthritis Rheum.* 41 (1998) 951–962.
- [13] A.W. Griffioen, A.F. Barendz-Janson, K.H. Mayo, H.F.P. Hillen, Angiogenesis, a target for tumor therapy, *J. Lab. Clin. Med.* 132 (1998) 363–368.
- [14] S. Dimmeler, A. Zeiher, Endothelial cell apoptosis in angiogenesis and vessel regression, *Circ. Res.* 87 (2000) 434–439.
- [15] A. Hayes, L. Li, M. Lippman, Antivascular therapy: a new approach to cancer treatment, *Br. Med. J.* 318 (1999) 853–856.
- [16] B. Olofsson, M. Jeltsch, U. Eriksson, K. Alitalo, Current biology of VEGF-B and VEGF-C, *Curr. Opin. Biotechnol.* 10 (1999) 528–535.
- [17] W. Schaper, I. Buschmann, VEGF and therapeutic opportunities in cardiovascular diseases, *Curr. Opin. Biotechnol.* 10 (1999) 541–543.
- [18] N. Ferrara, VEGF: an update on biological and therapeutic aspects, *Curr. Opin. Biotechnol.* 11 (2000) 617–624.
- [19] C. Jackson, M. Nguyen, J. Arkell, P. Sambrook, Selective matrix metalloproteinase (MMP) inhibition in rheumatoid arthritis—targeting gelatinase A activation, *Inflamm. Res.* 50 (2001) 183–186.
- [20] H. Kataoka, H. Itoh, M. Kono, Emerging multifunctional aspects of cellular serine proteinase inhibitors in tumor progression and tissue regeneration, *Path IT* 52 (2002) 89–102.
- [21] S. Desrivieres, H. Lu, N. Peyri, C. Soria, Y. Legrand, S. Menashi, Activation of the 92 kDa type IV collagenase by tissue kallikrein, *J. Cell. Physiol.* 157 (1993) 587–593.
- [22] H. Tschache, J. Michealis, U. Kohnert, J. Fedrowitz, R. Oberhoff, Tissue kallikrein effectively activates latent matrix degrading metalloenzymes, *Adv. Exp. Med. Biol.* 247A (1989) 545–548.
- [23] J. Plendl, C. Snyman, S. Naidoo, S. Sawant, R. Mahabeer, K.D. Bhoola, Expression of tissue kallikrein and kinin receptors in angiogenic microvascular endothelial cells, *J. Biol. Chem.* 281 (2000) 1103–1115.
- [24] K. Yayama, N. Kunitatsu, Y. Teranishi, M. Takano, H. Okamoto, Tissue kallikrein is synthesized and secreted by human vascular endothelial cells, *Biochim. Biophys. Acta* 1593 (2003) 231–238.
- [25] S. Naidoo, R. Ramsaroop, R. Bhoola, K.D. Bhoola, Correlation of kinin-generating activity with *Helicobacter pylori*-associated gastric infection, *Immunopharmacology* 43 (1999) 225–233.
- [26] K.D. Bhoola, C.D. Figueroa, K. Worthy, Bioregulation of kinins: kallikreins, kininogens and kininases, *Pharmacol. Rev.* 44 (1992) 1–80.
- [27] S. Naidoo, R. Ramsaroop, R. Bhoola, K.D. Bhoola, The evaluation of tissue kallikrein in *Helicobacter pylori*-associated gastric ulcer disease, *Immunopharmacology* 36 (1997) 263–269.
- [28] M. Schacter, Kallikreins (kininogenases)—a group of serine proteases with bioregulatory actions, *Pharmacol. Rev.* 31 (1980) 1–17.
- [29] D.F. Elliot, E.W. Horton, G.P. Lewis, Actions of pure bradykinin, *J. Physiol. (Lond.)* 153 (1960) 473–477.
- [30] R.H. Rixon, J.F. Whitfield, Kininogenases, Kallikrein, Schattauer-Verlag, Stuttgart, 1973.
- [31] J. Rehbock, P. Buchinger, A. Herman, C.D. Figueroa, Identification of immunoreactive tissue kallikrein in human ductal breast carcinomas, *J. Cancer Res. Clin. Oncol.* 121 (1995) 64–68.
- [32] Z. Dlamini, D.M. Raidoo, K.D. Bhoola, Tissue kallikrein and kinin receptors in oesophageal carcinoma, *Immunopharmacology* 43 (1999) 303–310.
- [33] T. Jones, C.D. Figueroa, C. Smith, D.R. Cullen, K.D. Bhoola, Characterization of a tissue kallikrein in human prolactin-secreting adenomas, *J. Endocrinol.* 124 (1990) 327–331.
- [34] D.M. Raidoo, S. Sawant, R. Mahabeer, K.D. Bhoola, Kinin receptors are expressed in human astrocytic tumour cells, *Immunopharmacology* 43 (1999) 255–263.
- [35] N. Koshikawa, H. Yasumitsu, M. Umeda, K. Miyazaki, Multiple secretion of serine proteinases by human gastric carcinoma cell lines, *Cancer Res.* 52 (1992) 5046–5053.
- [36] A. Stadnicki, J. Chao, I. Stadnicki, E. Van Tol, K.-F. Lin, F. Li, B. Sartor, R.W. Colman, Localization and secretion of tissue kallikrein in peptidoglycan-induced enterocolitis in Lewis rats, *Am. J. Physiol.* 275 (1998) G854–G861.
- [37] A. Stadnicki, U. Mazurek, M. Gonciarz, D. Plewka, G. Nowaczyk, J. Orchel, E. Pastucha, A. Plewka, T. Wilczok, R.W. Colman, Immunolocalization and expression of kallistatin and tissue kallikrein in human inflammatory bowel disease, *Dig. Dis. Sci.* 48 (2003) 615–623.
- [38] R. Miao, J. Agata, L. Chao, J. Chao, Kallistatin is a new inhibitor of angiogenesis and tumour growth, *Blood* 100 (2002) 3245–3252.
- [39] W. Wolf, D.M. Evans, L. Chao, J. Chao, A synthetic tissue kallikrein inhibitor suppresses cancer cell invasiveness, *Am. J. Pathol.* 159 (2001) 1797–1805.
- [40] R.W. Colman, R.A. Pixley, S. Najamunnisa, W. Yan, J. Wang, A.P. Mazar, K. McCrae, Binding of high molecular weight kininogen to human endothelial cells is mediated via a site within domains 2 and 3 of the urokinase receptor, *J. Clin. Invest.* 100 (1997) 1481–1487.
- [41] S. Asakura, R. Hurley, K. Skorstengaard, I. Ohkubo, D. Mosher, Inhibition of cell adhesion by high molecular weight kininogen, *J. Cell Biol.* 116 (1992) 465–476.
- [42] R.W. Colman, B.A. Jameson, Y. Lin, D. Johnson, S.A. Mousa, Domain 5 of high molecular weight kininogen (kininostat) down-regulates endothelial cell proliferation and migration and inhibits angiogenesis, *Blood* 95 (2000) 543–550.

- [43] J.-C. Zhang, K.P. Claffey, R. Sakthivel, Z. Darzynkiewicz, D. Shaw, J. Leal, Y.-C. Wang, F.-M. Lu, K. McCrae, Two-chain high molecular weight kininogen induces endothelial cell apoptosis and inhibits angiogenesis: partial activity within domain 5, *FASEB J.* 14 (2000) 2589–2600.
- [44] R.W. Colman, R. Pixley, I. Sainz, J. Song, I. Isordia-Salas, S. Muhamed, J. Powell, S.A. Mousa, Inhibition of angiogenesis by antibody blocking the action of proangiogenic high molecular weight kininogen, *J. Thromb. Haem.* 1 (2003) 164–170.
- [45] J.-C. Zhang, F. Donate, X. Qi, N. Ziats, J. Juarez, A.P. Mazar, Y.-P. Pang, K. McCrae, The antiangiogenic activity of cleaved high molecular weight kininogen is mediated through binding to endothelial cell tropomyosin, *Proc. Nat. Acad. Sci. U. S. A.* 99 (2002) 12224–12229.
- [46] M. Lukashev, Z. Werb, ECM signalling: orchestrating cell behaviour and misbehaviour, *Trends Cell Biol.* 8 (1998) 437–441.